On the correlation between the TiN thin film properties and the energy flux of neutral sputtered atoms in direct current magnetron discharge

Abderzak El Farsy, Jean-François Pierson, Thomas Gries, Ludovic de Poucques, Jamal Bougdira

On the correlation between the TiN thin film properties and the energy flux of neutral sputtered atoms in direct current magnetron discharge

On the correlation between the TiN thin film properties and the energy flux of neutral sputtered atoms in direct current magnetron discharge

Abderzak el Farsy[1,2,*], Jean-François Pierson[1], Thomas Gries[1], Ludovic de Poucques[1] , Jamal Bougdira[1]

[1] Université de Lorraine, CNRS, IJL, F-54000 Nancy, France.

[2] Université Paris-Saclay, CNRS, Laboratoire de Physique des Gaz et des Plasmas, 91405 Orsay, France.

*Corresponding author: abderzak.el-farsy@universite-paris-saclay.fr

Abstract:

In this study, the energy flux of sputtered atoms on a substrate was correlated to the properties of titanium nitride (TiN) films deposited using direct current magnetron sputtering (dcMS) under mixed Ar and N_2 atmospheres. The neutral titanium sputtered atoms velocity distribution functions (AVDFs) were measured by tunable diode-laser induced fluorescence (TD-LIF), and the flux of particles and their energy were derived. Mass spectrometry was used to characterize the energy-resolved flux of the ions. It was found that the neutral sputtered atoms flux and deposition rate were in good agreement, indicating that the flux of the neutral titanium ground state represents the number of deposited atoms. Moreover, TiN films were deposited at different gas pressures and at various Ar/N_2 gas mixtures close to the conditions where stoichiometric TiN was formed, without bias voltage and heating of the substrates. The energy flux of the sputtered neutral Ti into the substrate was calculated from TD-LIF measurements. At a relatively low magnetron discharge pressure of 0.4 Pa, we demonstrated that the energy of sputtered neutral Ti impinging on the substrate is higher than the energy flux of ionized particles corresponding mainly to Ar^+. Thus, the influence of the energy flux of the sputtered atoms on the texture and microstructure of the films is revealed. The (200) texture was obtained at 0.4 Pa when the energy flux of the sputtered atoms was higher than the ion energy flux. At 1.3 Pa where the sputtered atoms energy flux is one order lower compared to 0.4 Pa the (111) texture was obtained. The high-energy flux of the ground state of Ti sputtered atoms seems to allow stress removal in the films.

Keywords: dcMS, diode laser-induced fluorescence spectroscopy, TiN microstructure and texture.

I. Introduction

In magnetron sputtering (MS), the growth of polycrystalline thin films begins with vapor condensation on the substrate surface, which nucleates into islands and consolidates to form a continuous film. Thin films and coatings are used in a wide range of technological applications including microelectronics, optical devices, and surface protection. The performance of thin films and coatings depends on their physical properties, which are governed by film morphology and phase composition. These properties depend on the interactions of the particles with the substrate. Thus, the energy and flux of atoms and ions arriving at the substrate are of major importance for tailoring the forming film properties, such

as microstructure, stress, adhesion, electrical resistivity, stoichiometry, and crystalline properties. Titanium nitride (TiN) was used in this study because of its excellent mechanical and optical properties, and it has been used in several applications, such as decorative and wear-resistance [1,2].

Magnetron sputtering is a physical vapor deposition technique that can be operated with different power supplies: direct current magnetron sputtering (dcMS) to sputter conductive targets, radiofrequency magnetron sputtering primarily used to deposit dielectric materials, and high-power impulse magnetron sputtering (HiPIMS) [3,4]. In the dcMS process, most of the sputtered species remain in a neutral state, and their energy is controlled by the degree of thermalization, i.e., the number of collision events between the sputtered species and the processing gas. The number of collisions can be directly controlled by the deposition pressure and the target-to-substrate distance [5]. Their energy ranges from the energy they gain in the sputtering process and at virtually no collisions (~ 3.2 eV in average) to fully thermalized species at a larger number of collisions (~0.1 eV in average). Over the last two decades, HiPIMS has been intensively studied because of its ability to generate sputtered atoms with a high ionization rate (a few tens of percent). Such pulsed plasma discharges work at a peak current of approximately two orders of magnitude (low duty cycle: 1 % and low repetition frequency: < 5 kHz) compared with dcMS.

In conventional dcMS to deposit nitride thin films, the ion flux on the substrate mainly contains buffer gas ions (Ar^+ and N_2^+), whereas the sputtered species are mainly in a neutral state. For titanium nitride (TiN) deposition, the energy flux on the substrate, i.e., the product of particle flux and incident particle energy determines the growth mode. The TiN grains are preferentially oriented along the [111] direction for low energy flux, while [200] preferred orientation is observed for high energy flux [1,2,6,7]. Compared with ions, it is challenging to characterize energetic neutral-sputtered atoms. Their energy flux can be measured by mass spectrometry, a retarding field analyzer, and a Faraday cup, but the atoms must be ionized for detection [8]. Other devices have been developed and proposed to measure the energy flux towards the substrate surface without the ionization of incoming species as calorimetric probes [9–11]. In addition, both ions and neutral metallic flux towards the substrate were simulated by Mahieu and Depla [12] using the Monte Carlo approach of the SIMTRA code.

Tunable diode laser-induced fluorescence (TD-LIF) is a powerful technique for diagnosing neutral sputtered atoms with high spatial and spectral resolution, and the plasma remains practically unperturbed in terms of temperature and density [5,13–16]. Moreover, these measurements have numerous advantages compared to other optical diagnostics: (1) they allow probing of the ground state of the sputtered atoms in dcMS, (2) they are highly space and spectrally resolved, and (iii) they allow measurement of the flux and energy of sputtered atoms at the substrate position in front of the target. Other optical plasma diagnostics can be found in the literature, allowing the sputtered atom velocity distribution function (AVDFs) description [17–19].

Many previous works have studied TiN coatings deposited using either dcMS [1] or HiPIMS processes [6,7,20–22], and most of these studies investigated the impact of ion flux on the properties of TiN films. The present study aims to correlate the energy flux of neutral sputtered atoms on a substrate with the properties of TiN thin films (film texture, microstructure, and morphology) grown in dcMS discharges where the sputtered particles are mainly neutral. To achieve this goal, we used a balanced magnetron to reduce the ion flux on the substrate without bias and without intentional substrate heating. Thus, simultaneous measurements of TD-LIF and mass spectrometry of magnetron discharge

under different gas mixtures (Ar/N_2) were performed to characterize the energy flux of neutral sputtered Ti atoms and the ion energy flux, respectively.

II. Experimental details

The growth of TiN thin films and plasma diagnostics were carried out in a stainless-steel cylinder, 30 cm in diameter and 35 cm in height. Using mechanical and turbomolecular pumps, the base pressure obtained was approximately 2×10^{-4} Pa. A titanium target, 50 mm in diameter, 3 mm in thickness, and 99.99 % pure, was installed on a 2-inches balanced magnetron cathode cooled by water. The power source was a MELEC SIPP 2000 power supply (U_{max} =1 kV; I_{max_peak}= 200 A). The reactive gas mixture (Ar and N_2) was added to the chamber at various $N_2/(Ar+N_2)$ flow rate ratios, and the total flow rate was maintained at 18 sccm. We investigated the gas mixture range of 2 % to 5 % N_2 where quasi stochiometric TiN films were formed as shown latter by the measurements of the chemical composition of the films, the same conditions were found in early work with another deposition system [23]. For all the results presented in this work, the average power was fixed at 5 W cm^{-2} (100 W for the target area). In addition, all plasma measurements and thin film depositions were performed at a target-to-substrate distance of 5 cm (figure 1).

Plasma diagnostics and film depositions were performed in the same reactor, and the (100)-oriented Si substrates were installed using configuration 2, where the magnetron cathode was installed atop the chamber [figure 1 (b)]. No substrate bias or external heating was applied to the substrate during the film growth. The energy source on the substrate comes only from the deposited species, which are characterized by the diagnostic methods described below. Prior to deposition, all the substrates were ultrasonically cleaned in acetone for 10 min and ethanol for 10 min. Table 1 summarizes the deposition conditions.

Table 1. Summary of deposition conditions for the various realized coatings: reactive gas mixture, pressure, cathode voltage and film thickness.

% N_2		**2 %**	**3 %**	**5 %**
Deposition duration: 2 hours	**0.4 Pa**	345 V 3400 nm	340 V 3000 nm	351 V 2700 nm
	1.3 Pa	285 V 2600 nm	280 V 2800 nm	340 V 2300 nm

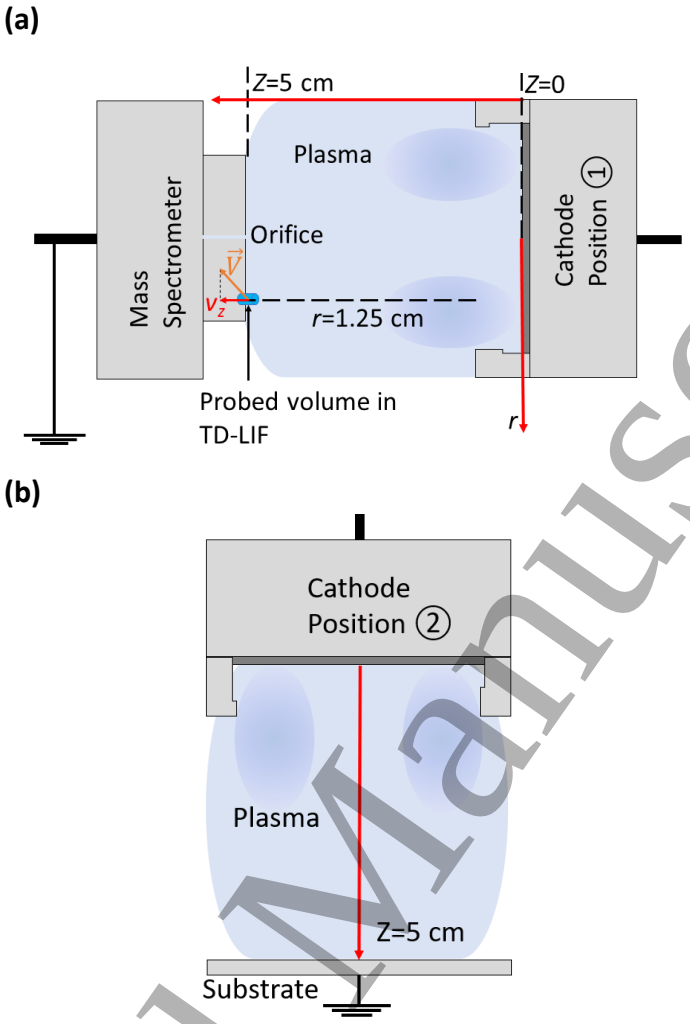

Figure 1. Schematic of the experimental setup. The cathode magnetron is in position ① to measure titanium neutral AVDFs and IEDFs, while it is moved to position ② atop the chamber to deposit thin films. The schemes are to scale. The measured atoms velocity by TD-LIF technique is the component v_z, for the sake of simplicity it is mentioned v in the text.

The velocity distribution functions of the neutral sputtered atoms were measured using the tunable diode laser-induced fluorescence technique (TD-LIF). The reader can refer to Desecures et *al.* [15] for a detailed description of the TD-LIF experimental setup. The laser source used in this study was a tunable diode laser (Toptica Photonics DL 100), which was accorded to probe the transition from $3d^2s^2$ ($^3F_2$) to $3d^2$ (^3F) $4s4p$ ($^1P^o$) of the ground state of neutral titanium sputtered atoms (λ_0=398.17 nm). The diode laser was tuned to scan a 9 pm wavelength range with a locked single-mode, and the spectral resolution was 0.005 pm, enabling an accurate description of the Doppler broadening profile. The typical scanning frequency for measurements was 50 Hz. The probed volume in the TD-LIF measurements was approximately 3 mm^3 above the racetrack center, that is, at r=1.25 cm and z = 5 cm (figure 1(a)). The combination of high spectral and spatial resolutions accurately measures the flux and energy of the deposited species.

The ion energy distribution functions (IEDFs) of Ar^+ and N_2^+ were measured using a HIDEN EQP 300 instrument. The plasma was sampled by a grounded orifice of a 100 μm diameter mass spectrometer installed in the virtual position of the substrate (figure 1(a)). Because the mass spectrometer signal depends on the differences in the acceptance angle for different ion energies and the unknown transfer function of the mass spectrometer, the measurements do not represent the absolute values of the ion flux; therefore, we discuss only the qualitative signal variations. Herein, only the qualitative changes in terms of energy are discussed. However, owing to the reactor geometry, mass spectrometry measurements were only performed in front of the target center at r= 0 cm (see figure 1).

The deposition rate was measured *via* scanning electron microscopy using a cross-sectional view of the specimens. The microstructure (crystallite size) and preferred orientation of the films were characterized by X-ray diffraction (XRD) analysis (Brüker D8 Advance with Cu K_α radiation, λ=1.54056 Å) in Bragg-Brentano geometry (θ-2θ). This mode allows for the identification of planes parallel to the thin-film surface. The chemical composition of the films was determined by wavelength dispersive X-ray spectroscopy (WDS), also known as electron probe microanalysis (EPMA), using a JEOL JXA-8530F instrument. Ti, Fe_4N, and MgO were used as standards to measure the Ti, N, and O concentrations, respectively. For each sample, the reported chemical composition was obtained by averaging 50 different spots measured on the surface (~ 200 × 200 μm^2). The topography and RMS roughness of the TiN films were investigated in resonant mode using a nano-observer atomic force microscope (AFM) developed by CSInstruments.

III. Results and discussion

III-1. Correlation between the deposited flux and deposition rate

Figure 2 shows the neutral Ti ($^3F_2$) AVDFs in dcMS discharge at 0.4 and 1.3 Pa, for the different gas mixtures (N_2/Ar). We used the resonance fluorescence signal ($\lambda_{laser} = \lambda_{lif}$ = 398.17 nm), which significantly improved the TD-LIF signal compared with previous studies [5,16]. Then, the AVDF profiles and the atoms populations are accurately described: thermalized (centered at v = 0 km/s) and energetic [v > 1 km/s ≈1 eV for titanium atoms] [5] are separated at relatively low and high magnetron pressures (p=0.4 and 1.3 Pa). The dashed curves represent fitting of the TD-LIF signal. The measured velocity field is the axial component (component perpendicular to the target surface as shown in figure 1 (a)), and two Gaussian functions were used to fit the experimental signal, which corresponded to the thermalized and energetic atoms populations. Because the measurements were carried out 5 cm away from the target, sputtered atoms undergo collision with the buffer gas, inducing the energetic population to be better fitted by a Gaussian function instead of the commonly known Thompson function [24]. The fitting by these two Gaussians results in some discrepancy for negative velocity (v < 0), especially at low pressure (0.4 Pa, top panel of figure 2). The main goal of the fitting is to better calculate the flux and energy of the atoms with momentum towards the substrate (positive velocity) to correlate with the film properties. Only the measurements performed at the substrate position are shown at a distance z = 5 cm from the target. For a detailed description of the AVDFs' fitting and titanium sputtered atoms transport characterization combined with PIC Monte Carlo modeling in argon gas, the reader is referred to Revel *et al.* [5].

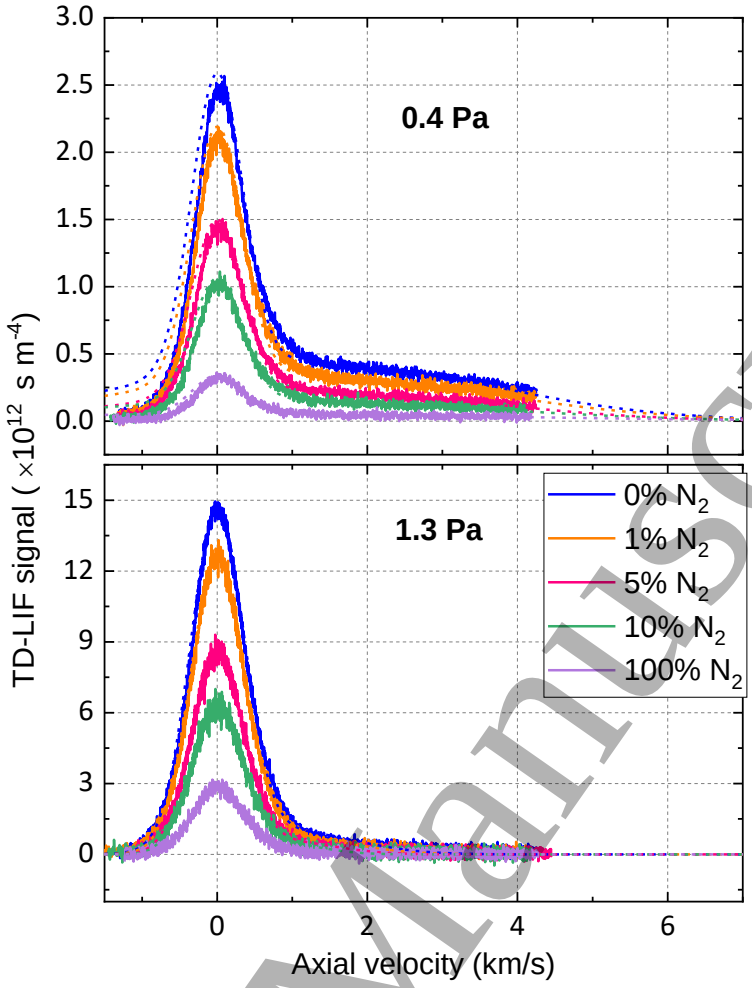

Figure 2. TD-LIF signal of the neutral Ti(J=2) atoms as a function of the percentage of N_2 in gas mixture at P_{DC}=5 W/cm^2, r=1.25 cm, z = 5 cm and p = 0.4 Pa (top) and p = 1.3 Pa (bottom). Dashed curves are the fitting of the measured signal.

The addition of nitrogen to the argon discharge completely altered the sputtering process. N_2 molecules react with the target surface material, forming a nitride layer that induces variations in secondary electron emission, electron temperature, and cathode voltage, but also induces variations in the ions striking the cathode, that is, Ar^+, N_2^+, and N^+ allowing sputtering instead of only Ar^+ in pure Ar gas. Figure 2 shows that the TD-LIF signal at the substrate positioned at a distance z = 5 cm from the target decreased progressively with increasing N_2 content. This decrease was observed for all atoms regardless of their energy. This is due to two main changes: (i) poisoning of the target surface in which the binding energy of Ti-N (8.04 eV [25]) is higher than that of Ti-Ti ones (6.6 eV [26]) and (ii) plasma variation in which the N^+ and N_2^+ ions can be less efficient for sputtering compared to the Ar^+ ion [27]. TD-LIF measurements performed near to the target surface (z= 1.1 cm) at low pressure of 0.4 Pa show that the surface nitridation affects the surface binding energy, we measured an average energy of 4.0±0.2 eV at nitride mode and 3.2±0.2 eV in metallic mode (100% Ar). The gas mixture does not affect the temperature of thermalized sputtered atoms since they are in thermal equilibrium with the buffer gas. In terms of the energy of the sputtered atoms, an expected difference can be observed when the gas pressure is increased; thermalized atoms are increased at a relatively high pressure (p=1.3 Pa)

compared to the energetic atoms. Indeed, the sputtered atoms leaving the target with an average energy of 4.0±0.2 eV (nitride mode, 3.2±0.2 eV in metallic mode) towards the substrate [5] undergo more collisions than at 0.4 Pa, efficiently transfer their energy to argon and nitrogen particles, and are more thermalized when they reach the substrate position at *p*=1.3 Pa.

We calculated the deposition rate from the film thickness determined from the scanning electron microscopy images. The flux of sputtered neutral Ti atoms ($^3F_2$, 0 eV) was obtained from the AVDFs using the following formula:

$$\Phi_{J=2}(\mathrm{cm^{-2}\ s^{-1}}) = \int_0^\infty v\ \mathrm{AVDF}(v)\ dv, \quad (1)$$

where, *v* is the axial velocity. Figure 3 (a) shows that the parameters, i.e., the flux of sputtered atoms and the deposition rate, are in good agreement.

Because the TD-LIF measurements were performed on the lower level of the ground state (*J* = 2), we assumed that neutral titanium atoms are in Boltzmann equilibrium and calculated the absolute value of the flux of ground-state titanium atoms as

$$\Phi_{\mathrm{absolute}}(\mathrm{cm^{-2}\ s^{-1}}) = \Phi_m \left\{1 + \sum_{J=1}^{m-1} \frac{g_J}{g_m} \exp\left(-\frac{E_J - E_m}{k_\mathrm{B}T}\right)\right\}, \quad (2)$$

where E_J and g_J are the energy and statistical weight, respectively, of state *J* and k_B is the Boltzmann constant. The titanium ground state has a triplet structure, in which the levels *J* = 2, 3, and 4 are at energies of 0, 0.021, and 0.047 eV, respectively. Therefore, Eq. (2) simplifies to

$$\Phi_{\mathrm{absolute}}(\mathrm{cm^{-2}\ s^{-1}}) = \Phi_{J=2} \left\{1 + \frac{g_3}{g_2} \exp\left(-\frac{E_3 - E_2}{k_\mathrm{B}T}\right) + \frac{g_4}{g_2} \exp\left(-\frac{E_4 - E_2}{k_\mathrm{B}T}\right)\right\}. \quad (3)$$

The temperature of the thermalized atoms was used to calculate the absolute flux of the Ti atoms. The absolute flux and deposition rates are shown in figure 3 (b). The flux of Ti atoms reaching the substrate at 2 % N_2 and *p* = 0.4 Pa was 6.8×10^{14} cm^{-2} s^{-1} and decreased to 5×10^{14} cm^{-2} s^{-1} when 5 % N_2 was added to the gas mixture. Similarly, the deposition rate decreased from 1700 to 1350 nm h^{-1} when the gas mixture varied from 2 to 5 % N_2. By increasing the pressure *p*= 1.3 Pa, a slight decrease in the deposition rate and Ti atoms flux was measured compared to *p*=0.4 Pa. The influence of the gas mixture was similar at both pressures. These variations show good agreement between the flux and the deposition rate for the 0.4 and 1.3 Pa pressures used in this work. In fact, increasing the percentage of nitrogen induces poisoning of the target and decreases the number of sputtered titanium atoms, resulting in a corresponding decrease in the deposition rate. In the studied pressure range, the pressure variation slightly affected the deposition rate, whereas the sputtered atoms thermalization increased significantly when the pressure increased (figure 2).

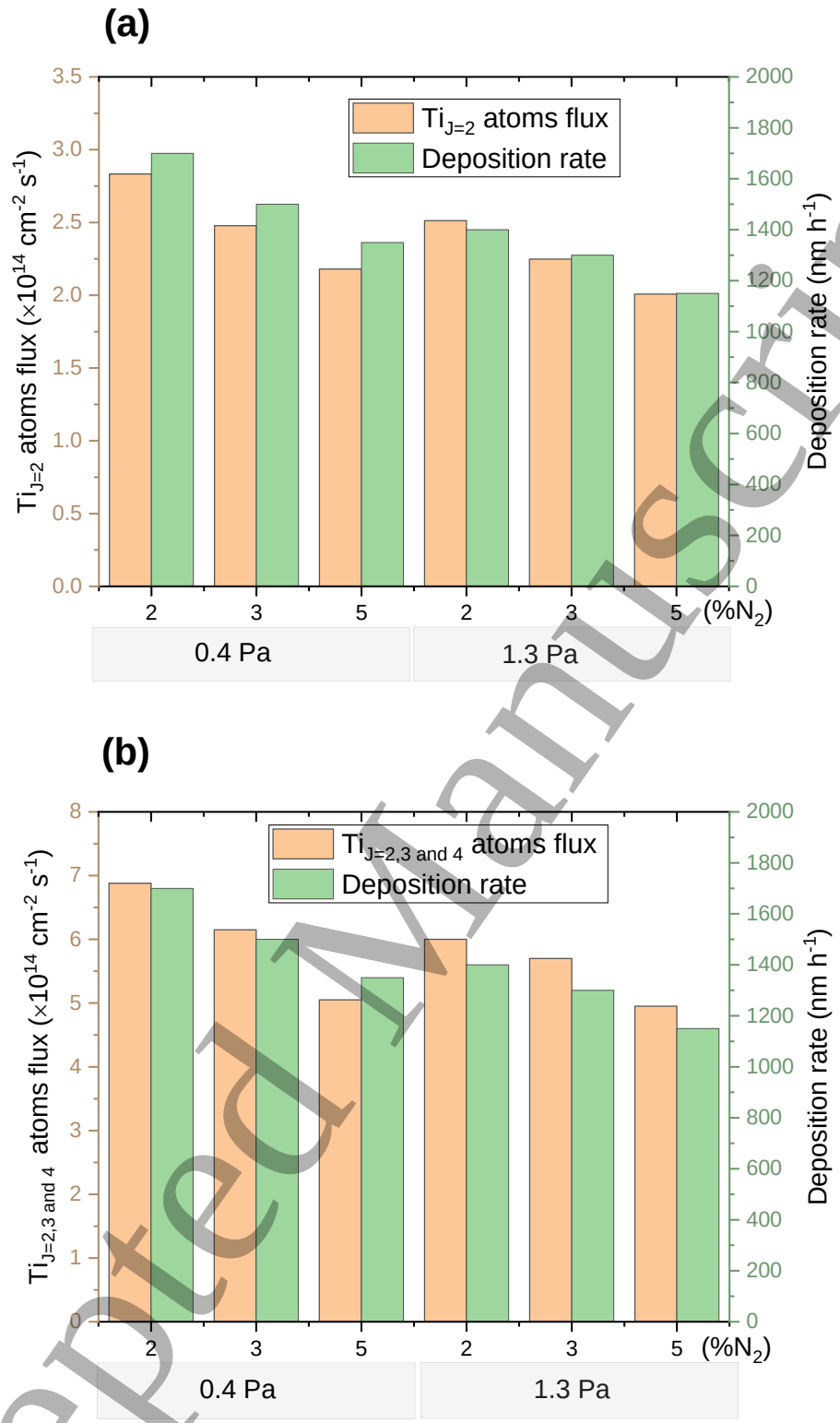

Figure 3. Variation of the flux of neutral Ti atoms [(a) J=2 level, (b) the absolute flux of neutral Ti] and the deposition rate under dcMS discharge as a function of the percentage of N_2 in the background gas at z = 5 cm, P_{DC} = 5 W cm^{-2}, and p = 0.4 and 1.3 Pa.

III-2. Influence of deposited energy on the film microstructure, texture, and morphology

As mentioned in the experimental section, TiN films were deposited in the dcMS discharge without any heating or bias of the substrate. The Ar gas temperature was measured as a function of the distance from the target using tunable diode laser absorption spectroscopy. It reaches a high temperature of 1400 K near the target (z = 1.3 cm), but a low temperature of approximately 500 K was measured at z = 5 cm [5]. Under these conditions, the total energy flux towards the substrate is the sum of the different contributions due to the kinetic energy of different deposited species. This section reports the different contributions.

In dcMS using a balanced magnetron, the plasma is trapped close to the target surface, in which the ion flux into the substrate decreases [4]. Figure 4 shows the IEDFs of Ar^+ and N_2^+ at 0.4 Pa and 3 %N_2 in gas mixture. The mass spectrometer signal represents the flux of ions, and two groups of ions arrive at the substrate: the low-energy group (E < 6 eV) and high-energy group (E around 20 eV). The low-energy group of ions is thermalized with the buffer gas. The high-energy group has been studied in many works, especially in HiPIMS discharge [28–30], and is generally attributed to ion acceleration inside spokes in magnetron plasma. As shown in figure 4, the signal magnitude of this high-energy group is three orders of magnitude lower than that of the thermalized ions. Thus, to calculate the energy flux towards the substrate, only low-energy ions were considered. In an early study of Ar/N_2 magnetron discharge, Petrov *et al.* [23] demonstrated that Ar^+ ions are the primary ions incident on the substrate in Ar-N_2 dcMS discharges, with a flux accounting for more than 92 % of the total ion flux when the percentage of N_2 was lower than 15 %. It worth to mention herein that ours mass spectrometer measurements are not calibrated. Thus, the corresponding ion energy flux to the substrate is calculated using the following expression [31]:

$$\Phi_{energy,\,Ar^+}(\,mW\ \mathrm{cm}^{-2}) = \frac{1}{4}\, e\, n_i v_i\, V \qquad (4)$$

where n_i and v_i are the ion density and thermal ion velocity, e is the electron charge and V is the voltage drop in the substrate sheath. Bradley et *al* [32] measured the ions density in dcMS with a cathode of 15 cm in diameter, 0.26 Pa argon pressure, and a dc power of about 1.5 W cm^{-2}, they found an ions density of about 10^{16} m^{-3} at z= 5 cm. In ours deposition system at z = 5 cm away from the target and P_{DC} =5 W cm^{-2}, we assumed an ion density of 2×10^{16} m^{-3} and an ion temperature of 600 K [5]. Based on our mass spectrometer measurements of the thermalized ions (figure 4), the voltage drop at the substrate sheath was estimated to be 3 V. For these plasma parameters, the energy flux corresponding to the ion contributions (equation 4) is approximately 0.075 mW cm^{-2}.

Regarding the energy flux of the electron contribution, the energetic secondary electrons accelerated in the cathode sheath are trapped near the cathode surface for ionization by the magnetic field, and only thermalized electrons can reach the substrate. Our substrate was grounded, and because the plasma potential at z = 5 cm was positive, the thermalized electrons were pushed away from the substrate. Therefore, their energy flux contributions can be neglected.

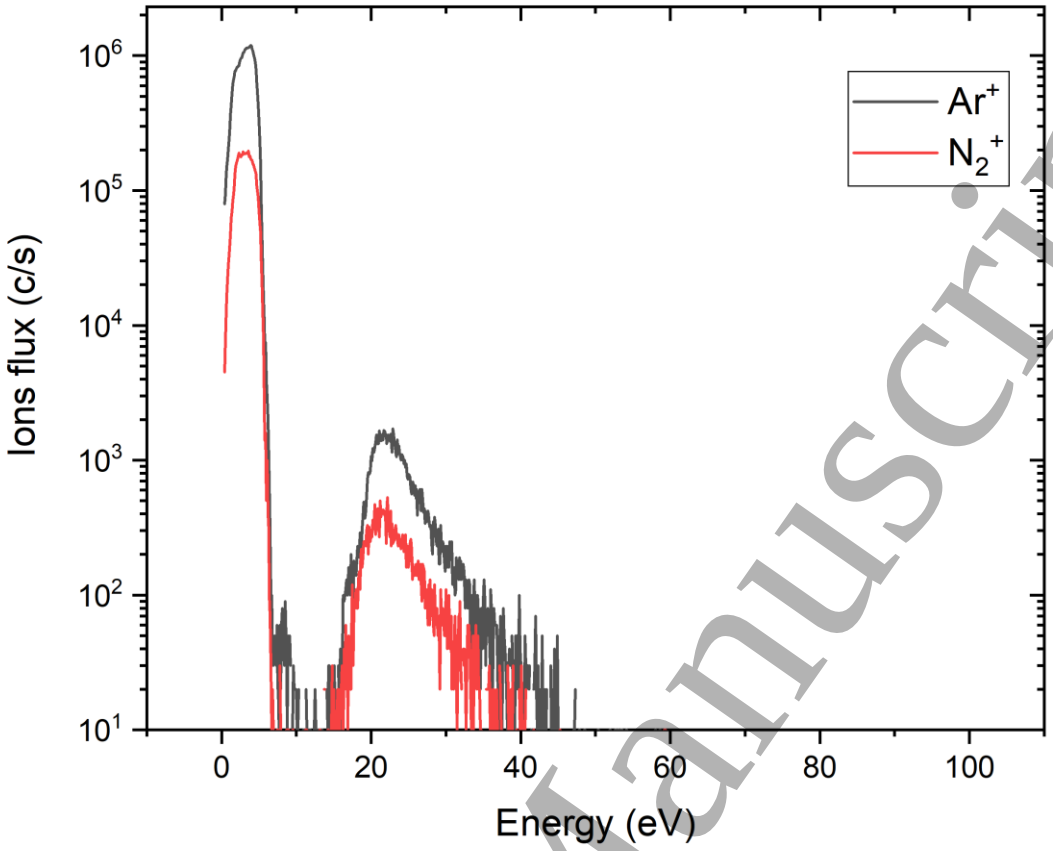

Figure 4. IEDFs of Ar^+ and N_2^+ ions at z = 5 cm, 3 % N_2, P_{DC} = 5 W cm^{-2}, and p = 0.4.

For the neutral species reaching the substrate, the energy flux deposited by Ti atoms (J=2) is obtained as follows:

$$\Phi_{energy,J=2} = \int_0^{\infty} \frac{1}{2} M\, v^2\, v\, \mathrm{AVDF}(v)\, \mathrm{d}v\,, \qquad (2)$$

where M (amu) is the atomic mass of titanium and v is the axial velocity. The total energy flux of the ground state Ti atoms was then deduced by applying equation (3). Figure 5 shows the variations in the energy flux of the ground state of the neutral Ti atoms and Ar^+ ions as a function of the nitrogen percentage. At p = 0.4 Pa, the energy flux gradually decreases from 0.27 to 0.20 mW cm^{-2} when the nitrogen percentage increases from 2 to 5 %. This decrease was mainly due to the decrease in the number of Ti-neutral atoms reaching the substrate. However, at p = 1.3 Pa, where the vapor is more thermalized, the energy flux is one order of magnitude lower than that measured at 0.4 Pa. It is on the order of 0.03 mW cm^{-2}. The most important result is that the energy flux of sputtered Ti atoms is higher than that of Ar^+ ions at a low magnetron pressure of 0.4 Pa. Other sputtered species, such as nitrogen atoms (N), could contribute to the energy flux towards the substrate, and its behavior as a function of pressure is expected to be similar to that of neutral Ti atoms. The knowledge of their energy flux requires further investigation. In other deposition system, Gauter *et al.* [33] used direct calorimetric probe to characterize the energy flux on the substrate during the deposition by HiPIMS

discharge with copper magnetron, they measured an averaged energy flux of 20 mW cm^{-2}. Calorimetric probe was also used by Bornholdt et al. [34] to energy flux during the deposition of ZnO by a radio-frequency discharge of 15 W cm^{-2} (3 target with 5 W cm^{-2}), they found a total energy flux of 30 mW cm^{-2}. In those calorimetric probe experiments, the energy flux is higher than the obtained by our diagnostics because (i) their measurements consider the contributions of all species arriving to the substrate, (ii) the discharge power is higher than used in our work and (iii) the zinc and copper have higher sputtering efficiency compared to titanium.

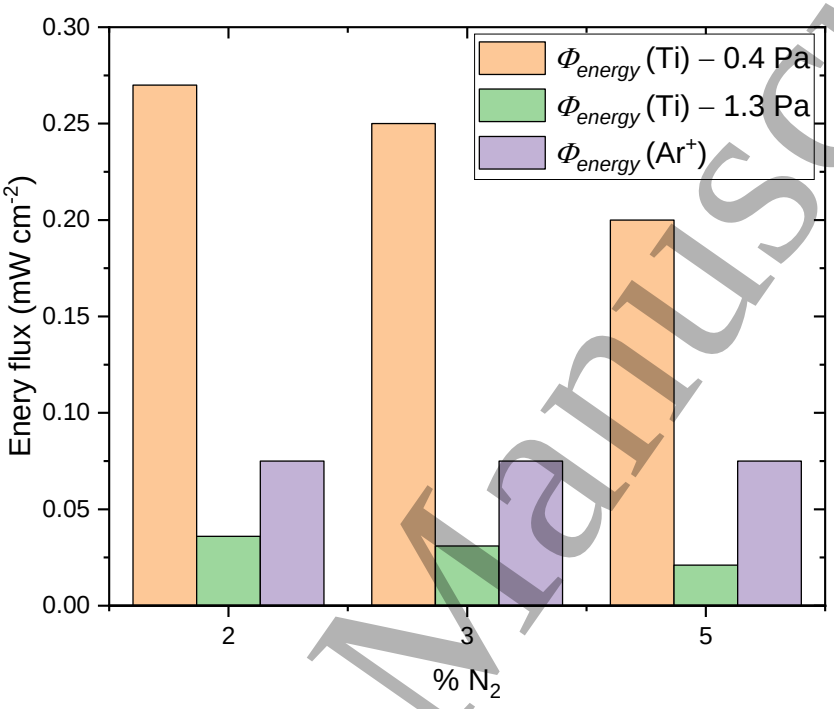

Figure 5. Energy flux of neutral of the ground state of Ti sputtered atoms as function of the percentage of N_2 in gas mixture, calculated at the substrate distance (z = 5 cm), for p = 0.4 and 1.3 Pa.

A. Film composition

Measurement of the chemical composition of thin films is not an easy task when the films contain light elements, such as nitrogen. The TiN samples deposited were analyzed using EPMA, and the percentages of O, Ti, and N were obtained. The quantitative results are summarized in Table 2. For Ti and N, the films are quasi-stoichiometric for both pressures (0.4 and 1.3 Pa). The Ti and N concentrations were approximately 48 and 50 at. % at respectively for the films at 0.4 Pa. At 1.3 Pa, the Ti concentration was 48 at. % and the N concentration is 46 at. %. Concerning the oxygen contamination, EPMA measurements show that the concentration of O element increases in the films from 2 at. % at 0.4 Pa to 6 at. % at 1.3 Pa. This contamination can be attributed to the residual oxygen in the chamber. Because the amount of oxygen in the chamber is constant and weak, the increase in oxygen concentration with the pressure is due to the decrease in the deposition rate. Indeed, films that grow at a low deposition rate contain more oxygen. However, the deposition rate at 1.3 Pa is about 85% of the deposition rate at 0.4 Pa. This decrease seems rather small to explain the increase of O concentration, from 2 to 6%. The higher oxygen concentration seems induced by film density (denser at 0.4 Pa)

or by the plasma variation especially the electron density and temperature assuming that the oxygen atoms are produced by the dissociation of oxygen molecule by electron impact.

Table 2. Concentration of Ti, N, and O elements measured with EPMA (top) for the samples deposited at 3%N_2.

	Ti	N	O
0.4 Pa	50 ±1 %	48 ±1 %	2 ±1 %
1.3 Pa	48 ±1 %	46 ±1 %	6 ±1 %

B. Film texture, microstructure, and morphology

Figure 6 shows the θ-2θ X-ray diffractograms of TiN films deposited in dcMS discharge for different gas mixtures at pressures of 0.4 and 1.3 Pa. All films exhibited characteristic diffraction peaks corresponding to polycrystalline TiN with a cubic (NaCl-type) structure. At 0.4 Pa, the thin films exhibit a mixed orientation with the (111) and (200) planes. Other planes with negligible intensities were detected and are not shown here. At 0.4 Pa, we observed that the (111) and (200) planes co-existed, but the peak corresponding to the (200) planes was highly dominant. At 1.3 Pa, we observed that the (111) planes exhibited the highest intensity for all percentages of N_2 investigated. We also observed the quasi-absence of the (200) planes. The two preferred orientations have different surface energies. In fact, the family of (111) planes has an atom density greater than that of (200) planes, thus inducing a lower surface energy of the (111) planes. Therefore, we can consider that the latter are more stable and require less energy to be produced than the (200) plane. Thus, the preferred (111) orientation is the result of deposition under conditions close to equilibrium [6]. Because the TiN films were deposited at ambient temperature and without substrate bias, the texture variation could only be affected by the energy flux of the arriving species and the chemical composition of the films.

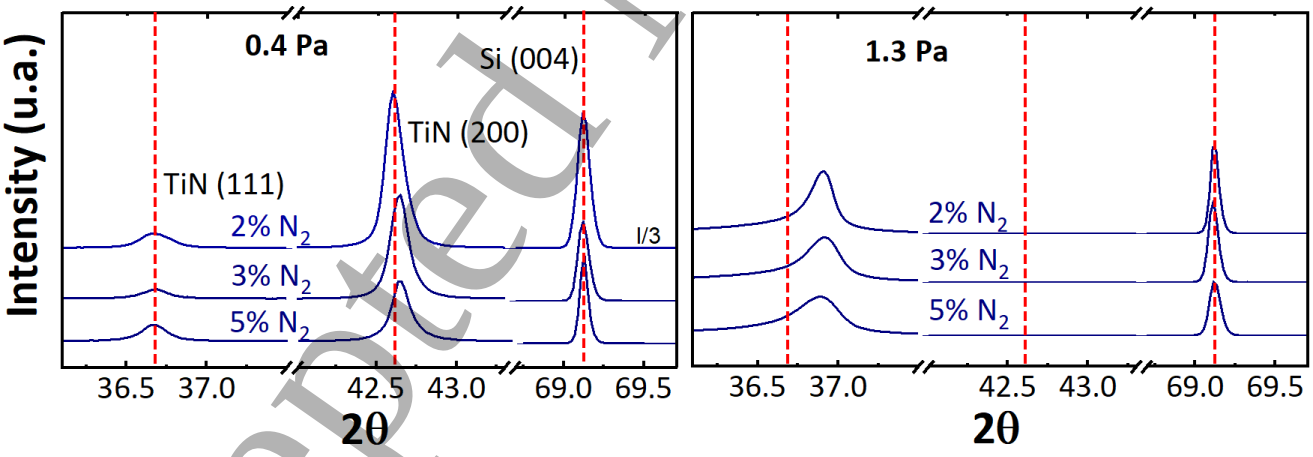

Figure 6. θ-2θ X-ray diffractograms of TiN films deposited by dcMS as a function of the percentage of N_2 in the gas mixture, at p = 0.4 Pa (left) and 1.3 Pa (right). For films at p = 0.4 Pa — 2 % N_2 the XRD signal was divided by a factor of 3.

The gas composition and total pressure influence the number of sputtered Ti neutral atoms reaching the substrate position (figure 3) and substantially affect the energy flux of neutral-sputtered Ti atoms (figure 5). It should be noted that films with similar chemical compositions have different preferred

orientations. The preferred orientation has been studied in many previous works on dcMS under different energetic ion bombardment conditions [6,35–37], and it is well known that by increasing the ion energy at the substrate, the preferred orientation switches from [111] to [200]. As shown in figure 5, at a low pressure (0.4 Pa) we found that the energy flux of the ion contribution towards the substrate is negligible, and the primary deposited energy that can affect the adatom is the energy flux of the ground state of neutral Ti sputtered atoms. As the switching of preferred orientation from the [200] to the [111] one occurs by switching the pressure from 1.3 to 0.4 Pa, we deduce that the energy flux of the neutral sputtered species (Ti and N) enables the growth of films with [200] orientation. The (200) preferred orientation is characterized by high hardness compared with the [111] orientation [7,20].

Using X-ray diffractograms, the (111) and (200) peaks were adjusted using a Lorentzian function, and the full width at half maximum (FWHM) was determined to estimate the crystallite size based on the Scherrer formula [38]. The (111) peaks at 1.3 Pa were fitted with two Lorentzian functions because of the asymmetry on the left of the peak, and the crystallite size was calculated from the FWHM of the Lorentzian with the highest amplitude. The results are shown in figure 7 (a). There are two groups of crystallites according to their size. A group of sizes of approximately 18 ± 2 nm corresponding to the crystallites oriented in the [100] direction normal to the substrate existing in the films at 0.4 Pa. The second group had a crystallite size of approximately 5 ± 2 nm among the remaining crystallites. Recently, Viloan et *al.* [20] reported a high hardness of TiN crystallites with a large crystallite size. This type of crystallite is obtained when the energy flux of the sputtered neutral is higher than the energy flux of the ion contribution (figure 5).

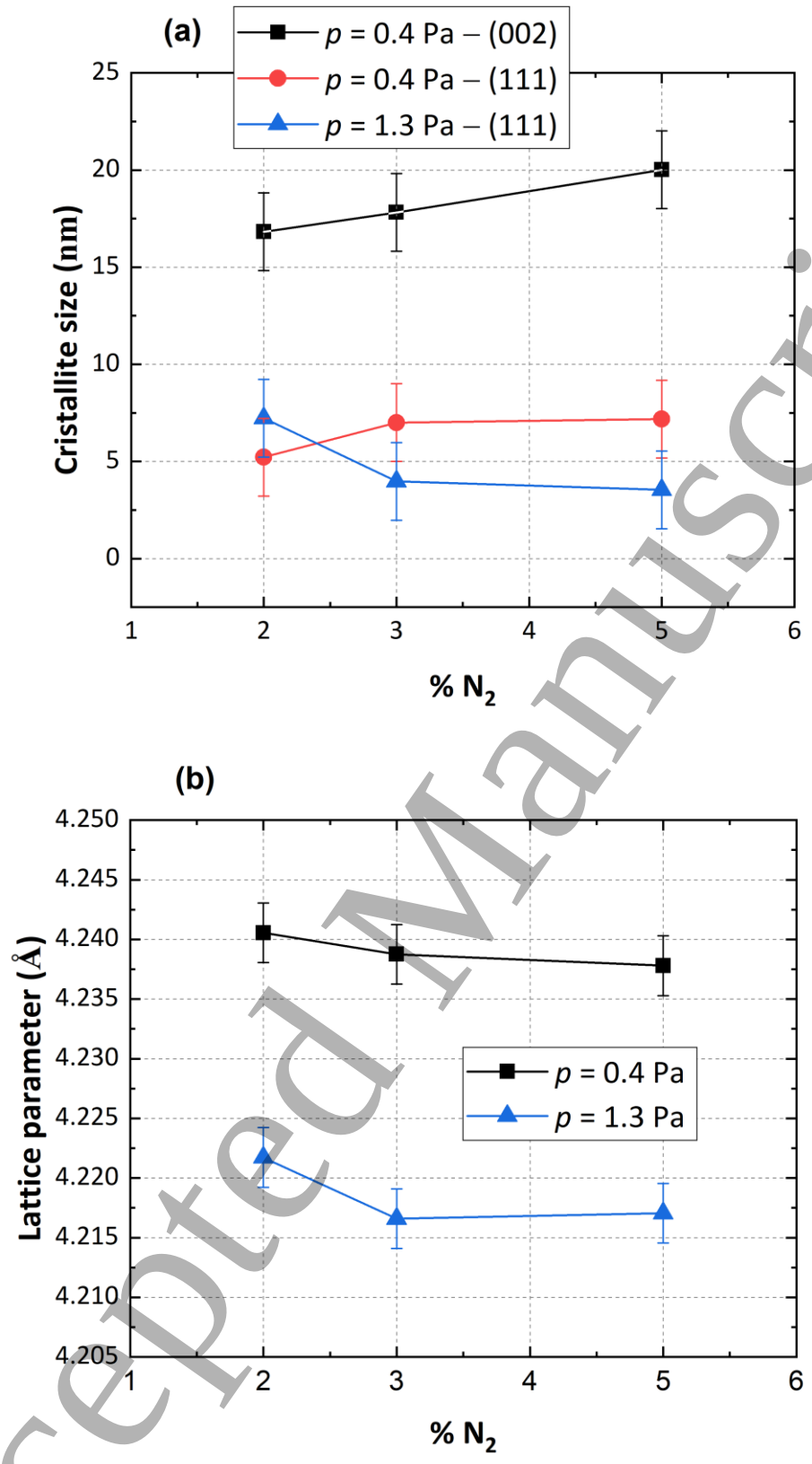

Figure 7. Variations of crystallite size (a) and lattice parameter (b) as function of the percentage of N_2 in the gas mixture, in dcMS process.

Similarly, peak fitting was used to calculate the lattice parameter, considering the shift in the

diffraction angle in the Bragg equation [figure 7 (b)]. This was possible because the calibration of the XRD instrument was performed using the (004) diffraction peak observed from the Si substrate for all samples (figure 6). The films deposited at 0.4 Pa exhibit a lattice constant around 4.24 Å. The lattice constant of bulk TiN is 4.24 Å in the absence of stress. An increase in the nitrogen ratio in the gas mixture from 2 % to 5 % induced a slight decrease in the lattice constant from 4.240 Å to 4.235 Å. This decrease may be related to a slight variation in the concentration of N in the film, which was not detected by EPMA. However, for the films deposited at 1.3 Pa the lattice parameter was approximately 4.215 Å, suggesting the presence of tensile stress in the films. As shown in figure 4, the energy flux of sputtered Ti atoms at 0.4 Pa is one order of magnitude higher than at 1.3 Pa. Therefore, the high-energy flux of Ti atoms seems to allow stress removal in films at low pressures.

AFM measurements were performed to determine the morphology and roughness of the film surfaces (figure 8). The films deposited at 0.4, 1.3 Pa, and 3 % N_2 with approximately similar thicknesses (~ 2.9 μm) were characterized. The film deposited at low pressure exhibited a very high roughness (RMS surface roughness = 67 nm). The surface of this film showed large faceted grains, in agreement with the XRD results. On the other hand, the film deposited at 1.3 Pa show a lower roughness (RMS surface roughness = 11 nm) and small grains. Once again, the difference in the film surface morphology may be explained by the high energy flux of sputtered Ti atoms at 0.4 Pa.

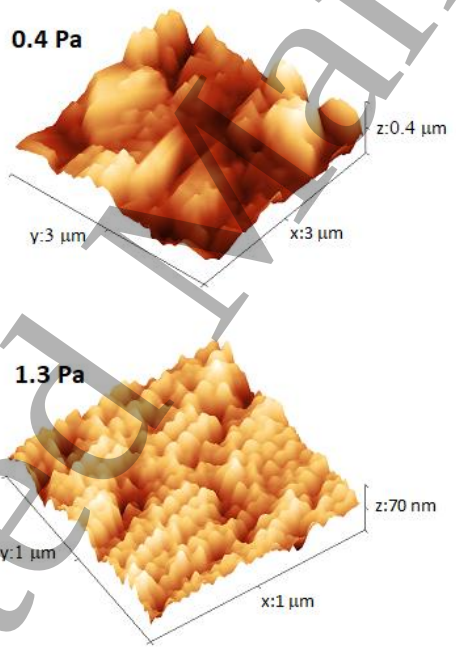

Figure 8. AFM images of the surface of the samples deposited in dcMS, at 2 % N_2 in the gas mixture and p = 0.4 Pa (top) and 1.3 Pa (bottom).

IV. Conclusion

The neutral titanium sputtered atoms velocity distribution functions (AVDFs) at the substrate position were measured by a tunable diode laser induced fluorescence (TD-LIF) technique in direct current

magnetron sputtering (dcMS) discharge and correlated to the TiN thin film properties. The measured velocity was perpendicular to the substrate (axial velocity in a planar circular magnetron). The flux of the sputtered particles was then calculated and correlated with the deposition rate. Their evolutions as a function of the N_2 content in the gas mixture are in good agreement. TiN thin films were deposited at 0.4 and 1.3 Pa, for different gas mixtures Ar/N_2 close to the conditions where stoichiometric TiN was formed, without bias voltage and heating of the substrates. Their microstructure, texture, and chemical composition were characterized using X-ray diffraction, EPMA. The films deposited at a low pressure (0.4 Pa) show a [200] preferred orientations. For 1.3 Pa, the films were oriented along the [111] direction and tensile stress was observed. Because the film growth was carried out without bias and heating of the substrate, we studied the influence of the energy flux (i.e., the product of particle flux and incident particle energy) of sputtered atoms deduced from TD-LIF measurements on the film properties. At a relatively low magnetron discharge pressure of 0.4 Pa, we found that the energy of the ground state of sputtered neutral Ti impinging on the substrate is higher than the energy flux of ionized particles corresponding mainly to Ar^+. This high energy flux of sputtered neutral atoms allows the growth of TiN oriented along the [111] direction. In addition, it allows stress removal in the films. At 1.3 Pa where the sputtered atoms energy flux is one order lower compared to 0.4 Pa the (111) texture was obtained.

Acknowledgments

The authors thank Mrs. Christine Gendarme and Mr. Denis Mangin from the Centre de Compétences 3M of the Institut Jean Lamour for WDS analyse. The Centre de Compétences X-γ of the Institut Jean Lamour is also acknowledged for the access to the X-ray diffractometers.

References

[1] Abadias G, Leroy W P, Mahieu S and Depla D 2012 Influence of particle and energy flux on stress and texture development in magnetron sputtered TiN films *J. Phys. D: Appl. Phys.* **46** 055301

[2] Wang Z, Zhang D, Ke P, Liu X and Wang A 2015 Influence of Substrate Negative Bias on Structure and Properties of TiN Coatings Prepared by Hybrid HIPIMS Method *Journal of Materials Science & Technology* **31** 37–42

[3] Depla D, Mahieu S and Greene J E 2010 *Handbook of deposition technologies for films and coatings: science, applications and technology* ed P M Martin (Amsterdam: Elsevier)

[4] Anders A 2017 Tutorial: Reactive high power impulse magnetron sputtering (R-HiPIMS) *Journal of Applied Physics* **121** 171101

[5] Revel A, Farsy A E, de Poucques L, Robert J and Minea T 2021 Transition from ballistic to thermalized transport of metal-sputtered species in a DC magnetron *Plasma Sources Sci. Technol.* **30** 125005

[6] Ehiasarian A P, Vetushka A, Gonzalvo Y A, Sáfrán G, Székely L and Barna P B 2011 Influence of high power impulse magnetron sputtering plasma ionization on the microstructure of TiN thin films *Journal of Applied Physics* **109** 104314

[7] Cemin F, Abadias G, Minea T and Lundin D 2019 Tuning high power impulse magnetron sputtering discharge and substrate bias conditions to reduce the intrinsic stress of TiN thin films *Thin Solid Films* **688** 137335

[8] Benedikt J, Kersten H and Piel A 2021 Foundations of measurement of electrons, ions and species fluxes toward surfaces in low-temperature plasmas *Plasma Sources Sci. Technol.* **30** 033001

[9] Stahl M, Trottenberg T and Kersten H 2010 A calorimetric probe for plasma diagnostics *Review of Scientific Instruments* **81** 023504

[10] Abolmasov S N, Cormier P A, Torres Rios A, Dussart R, Semmar N, Thomann A L and Roca i Cabarrocas P 2012 Probing dusty-plasma/surface interactions with a heat flux microsensor *Appl. Phys. Lett.* **100** 011601

[11] Trottenberg T and Kersten H 2017 Measurement of forces exerted by low-temperature plasmas on a plane surface *Plasma Sources Sci. Technol.* **26** 055011

[12] Mahieu S and Depla D 2009 Reactive sputter deposition of TiN layers: modelling the growth by characterization of particle fluxes towards the substrate *J. Phys. D: Appl. Phys.* **42** 053002

[13] Farsy A E, Ledig J, Desecures M, Bougdira J and Poucques L de 2019 Characterization of transport of titanium neutral atoms sputtered in Ar and Ar/N2 HIPIMS discharges *Plasma Sources Sci. Technol.* **28** 035005

[14] Desecures M, de Poucques L, Easwarakhanthan T and Bougdira J 2014 Characterization of energetic and thermalized sputtered atoms in pulsed plasma using time-resolved tunable diode-laser induced fluorescence *Applied Physics Letters* **105** 181120

[15] Desecures M, Poucques L de and Bougdira J 2014 Characterization of energetic and thermalized sputtered tungsten atoms using tuneable diode-laser induced fluorescence in direct current magnetron discharge *Plasma Sources Science and Technology* **24** 015012

[16] Vitelaru C, Aniculaesei C, de Poucques L, Minea T M, Boisse-Laporte C, Bretagne J and Popa G 2010 Tunable diode-laser induced fluorescence on Al and Ti atoms in low pressure magnetron discharges *Journal of Physics D: Applied Physics* **43** 124013

[17] Held J, Hecimovic A, von Keudell A and Schulz-von der Gathen V 2018 Velocity distribution of titanium neutrals in the target region of high power impulse magnetron sputtering discharges *Plasma Sources Science and Technology* **27** 105012

[18] Britun N, Palmucci M and Snyders R 2011 Fast relaxation of the velocity distribution function of neutral and ionized species in high-power impulse magnetron sputtering *Applied Physics Letters* **99** 131504

[19] Fekete M, Hnilica J, Vitelaru C, Minea T and Vašina P 2017 Ti atom and Ti ion number density evolution in standard and multi-pulse HiPIMS *Journal of Physics D: Applied Physics* **50** 365202

[20] Viloan R P B, Lundin D, Keraudy J and Helmersson U 2020 Tuning the stress in TiN films by regulating the doubly charged ion fraction in a reactive HiPIMS discharge *Journal of Applied Physics* **127** 103302

[21] Ghailane A, Larhlimi H, Tamraoui Y, Makha M, Busch H, Fischer C B and Alami J 2020 The effect of magnetic field configuration on structural and mechanical properties of TiN coatings deposited by HiPIMS and dcMS *Surface and Coatings Technology* **404** 126572

[22] Ghailane A, Oluwatosin A O, Larhlimi H, Hejjaj C, Makha M, Busch H, Fischer C B and Alami J 2022 Titanium nitride, TiXN(1−X), coatings deposited by HiPIMS for corrosion resistance and wear protection properties *Applied Surface Science* **574** 151635

[23] Petrov I, Myers A, Greene J E and Abelson J R 1994 Mass and energy resolved detection of ions and neutral sputtered species incident at the substrate during reactive magnetron sputtering of Ti in mixed Ar+N2 mixtures *Journal of Vacuum Science & Technology A* **12** 2846–54

[24] Stepanova M and Dew S 2004 *Nucl. Instrum. Methods Phys. Res. B* **215** 357–365

[25] Luo Y-R 2007 *Comprehensive handbook of chemical bond energies.* (CRC press)

[26] Du L, Edgar J H, Peascoe-Meisner R A, Gong Y, Bakalova S and Kuball M 2010 Sublimation crystal growth of yttrium nitride *Journal of Crystal Growth* **312** 2896–903

[27] Rossnagel S M 2003 Thin film deposition with physical vapor deposition and related technologies *Journal of Vacuum Science & Technology A: Vacuum, Surfaces, and Films* **21** S74–87

[28] Maszl C, Breilmann W, Benedikt J and von Keudell A 2014 Origin of the energetic ions at the substrate generated during high power pulsed magnetron sputtering of titanium *Journal of Physics D: Applied Physics* **47** 224002

[29] Hecimovic A 2016 Anomalous cross-Bfield transport and spokes in HiPIMS plasma *J. Phys. D: Appl. Phys.* **49** 18LT01

[30] El Farsy A, Boivin D, Noel C, Hugon R, Cuynet S, Bougdira J and de Poucques L 2021 Ionized particle transport in reactive HiPIMS discharge: correlation between the energy distribution functions of neutral and ionized atoms *Plasma Sources Sci. Technol.* **30** 065016

[31] Bornholdt S, Fröhlich M and Kersten H 2014 Calorimetric Probes for Energy Flux Measurements in Process Plasmas *Complex Plasmas* Springer Series on Atomic, Optical, and Plasma Physics vol 82, ed M Bonitz, J Lopez, K Becker and H Thomsen (Cham: Springer International Publishing) pp 197–234

[32] Bradley J W, Thompson S and Gonzalvo Y A 2001 Measurement of the plasma potential in a magnetron discharge and the prediction of the electron drift speeds *Plasma Sources Sci. Technol.* **10** 490–501

[33] Gauter S, Fröhlich M and Kersten H 2018 Direct calorimetric measurements in a PBII and deposition (PBII&D) experiment with a HiPIMS plasma source *Surface and Coatings Technology* **352** 663–70

[34] Bornholdt S, Itagaki N, Kuwahara K, Wulff H, Shiratani M and Kersten H 2013 Characterization of the energy flux toward the substrate during magnetron sputter deposition of ZnO thin films *Plasma Sources Sci. Technol.* **22** 025019

[35] Cemin F, Tsukamoto M, Keraudy J, Antunes V G, Helmersson U, Alvarez F, Minea T and Lundin D 2018 Low-energy ion irradiation in HiPIMS to enable anatase TiO2 selective growth *J. Phys. D: Appl. Phys.* **51** 235301

[36] Magnus F, Ingason A S, Sveinsson O B, Olafsson S and Gudmundsson J T 2011 Morphology of TiN thin films grown on SiO2 by reactive high power impulse magnetron sputtering *Thin Solid Films* **520** 1621–4

[37] Viloan R P B, Gu J, Boyd R, Keraudy J, Li L and Helmersson U 2019 Bipolar high power impulse magnetron sputtering for energetic ion bombardment during TiN thin film growth without the use of a substrate bias *Thin Solid Films* S0040609019303621

[38] Elmkhah H, Attarzadeh F, Fattah-alhosseini A and Kim K H 2018 Microstructural and electrochemical comparison between TiN coatings deposited through HIPIMS and DCMS techniques *Journal of Alloys and Compounds* **735** 422–9